Infrared measurement of thermal constants in laser irradiated scleral tissue

Jamie D. Rhead, Aravinda Kar, and Glenn D. Boreman

Center for Research and Education in Optics and Lasers
University of Central Florida, Orlando, FL 32816

Fabrice Manns, Mikio Sasoh, and Jean-Marie Parel

Bascom Palmer Eye Institute
University of Miami School of Medicine, Miami, FL 33136

ABSTRACT

Laser scleral buckling (LSB) experiments were performed by irradiating human cadaver eyes with a focused beam from a 2.1-μm Ho:YAG laser. Spatially and temporally resolved temperature maps of the sclera were inferred from infrared images of the tissue's thermal radiation. An infrared focal-plane camera operating in the 3- to 5-μm wavelength interval was used for the measurements, from which we derived absorption and thermal diffusivity coefficients of the scleral tissue, along with the temperature dependence of these coefficients. A thermal-response model was developed, which describes the tissue surface temperature in response to a train of laser pulses, given the pulse repetition rate, beam fluence, spot size, and total energy delivered. This model provides guidance for optimization of laser-irradiation parameters for LSB treatment.

Key words: absorption, collagen, infrared, laser heating, retinal detachment, thermal diffusivity

1. INTRODUCTION

Laser scleral buckling (LSB) is an experimental procedure for treating retinal detachment where a scleral indentation is created by laser-induced scleral collagen shrinkage.[1] The collagen fibers of the sclera shrink at a temperature[2] of 60 to 70°C and recent research[3] has demonstrated that effective collagen contraction can occur at temperatures as high as 80°C. A pulsed Holmium:YAG (2.1 μm) or Thulium:YAG laser (2.01 μm) can generate the required temperature increase sufficiently deep within the sclera to create a significant indentation effect.[4] However, the energy per pulse and the total energy applied to the sclera must be controlled precisely to avoid overheating of the superficial sclera or thermal damage to the choroid and retina. To determine the energy required to create both an efficient and safe scleral heating, the temperature distribution generated at the surface and inside the sclera must be known.

Measurements with infrared-imaging techniques of the surface temperature of the sclera during pulsed laser scleral heating are presented. Based on these measurements, the scleral absorption coefficient and thermal diffusivity are determined, and we derive a thermal model for LSB. The model gives the temperature distribution in the sclera as a function of laser parameters (peak fluence, spot size, repetition rate, and number of pulses). Surface and volume temperature distributions are generated from this model to help determine the appropriate laser parameters for performing laser scleral buckling.

2. MATERIALS AND METHODS

2.1. Imaging system

The optical setup is shown in Fig. 1. Infrared images were taken with a Mitsubishi 5120A thermal camera used with an electronic gain of 2 and an f-number of 3.2. A relay lens system was used with the infrared camera to provide a magnification of -0.5. As the detector was a 512-by-512 array of platinum-silicide detectors with a spacing of 22 μm, the optical system allowed the observation of a 2.25×2.25 cm square area with a spatial resolution of 44 μm. The thermal camera produced 512×512 data arrays of 8-bit pixels. The images were recorded using a Panasonic AG-6300 video cassette recorder, were extracted with a frame grabber at 30 frames/s, and were processed on a Sun workstation with IDL software.

Conversion of the images to temperature distributions was performed by comparison with flat-field calibration data from a CI Systems SR-80-4D extended-area blackbody. Video recordings of the source were made from 25 to 100°C in 5°C intervals. At each temperature, the radiation source was recorded for 30 s, and a calibration image was generated by averaging several frames. A single pixel value could not be used to characterize each temperature for the entire field of view because the detector array and relay lens system of the infrared imager produced a nonuniform response. To remove this shading effect, experimental data were processed into temperature distributions by interpolation between the sixteen calibration images on a pixel-by-pixel basis. This is equivalent to calibrating each detector independently. An image processed in this way has the nonuniform response of the system removed, leaving for each pixel value the actual temperature seen by a particular element of the detector.

2.2. Preparation of the eyes

Fresh human cadaver eyes donated by the Florida Lions Eye Bank were used for these studies. Globes with scleral or other ocular abnormalities and eyes that had a previous surgical procedure (e.g., keratoplasty, cataract surgery, vitrectomy) were discarded. Using an operation microscope, the globes were denuded of remaining conjunctiva with a scalpel. No attempt was made to remove Tenon's capsule. The globes were bisected through the antero-posterior optical axis and the iris, ciliary body, crystalline lens, vitreous and retinal-choroidal layers were removed. Scleral shells showing clinical signs of pathologies were discarded. The half scleral shells were immersed in saline solution (BSS, Alcon Inc., Fort Worth) for storage prior to laser treatment, as this solution was shown to maintain the sclera degree of hydration within normal physiological range (Sasoh et al. unpublished experiments). For treatment, the shells were suspended and attached to the optical setup using 4-0 silk sutures. The thickness of all scleral shells used in these studies were physiologically normal. No attempt was made to raise the tissues to body temperature (≈ 36°C) and all experiments were performed at room temperature (22 ± 2°C).

2.3. Experiments

The eyes were irradiated with a pulsed Ho:YAG laser (2.1 μm, 250 μs, 5 Hz, 0-200 mJ) from Sunrise Technologies. The laser output was delivered through a 400-μm low-OH optical fiber. The fiber end was imaged at the equator of the sclera with a calcium-fluoride lens. The beam width was varied from 2.3 to 2.7 mm and was measured with thermal paper. Twenty-five trials were performed in which the number of pulses on the sclera was varied from 1 to 100. The energy per pulse was measured with a Molectron JD 500 Joulemeter.

Data in this paper were taken from three trials in which 23 pulses were applied to the sclera. The output of the fiber was imaged at the equator of the sclera to a 2.7-mm-diameter spot. The irradiance distribution was approximately Gaussian. The energy per pulse was measured to be 144 mJ. The average fluence per pulse was determined by dividing the energy per pulse by the beam area to be $I_{avg} = 2.5$ J cm^{-2}. The laser was applied normally to the scleral surface and the camera was positioned to image the sclera at a 20° horizontal angle as shown in Fig. 1. Foreshortening in the image was corrected by dividing the image scale by $\cos(20°) \approx 0.94$ in the horizontal direction.

3. THERMAL MODEL

3.1. Heat-transfer equation

The differential equation of heat conduction in cylindrical coordinates for a homogenous, isotropic, non-scattering tissue irradiated with a laser is given by[5]

$$\frac{\partial^2 T}{\partial r^2} + \frac{1}{r}\frac{\partial T}{\partial r} + \frac{\partial^2 T}{\partial z^2} + \frac{\mu}{k} E(r,t)\exp(-\mu z) = \frac{\rho c}{k}\frac{\partial T}{\partial t} = \frac{1}{\alpha}\frac{\partial T}{\partial t} \tag{1a}$$

where $T = T(r,z,t)$ is the temperature of the tissue, k is the thermal conductivity (W cm^{-1} °C^{-1}), ρ is the density (g cm^{-3}), c is the heat capacity (J g^{-1} °C^{-1}), μ is the absorption coefficient (cm^{-1}), α is the thermal diffusivity (cm^2 s^{-1}), and $E(r,t)$ is the irradiance (W cm^{-2}). For a Gaussian beam, the irradiance is given by

$$E(r,t) = \frac{2}{\pi w^2} P(t) \exp\left(-2 r^2 / w^2\right) \tag{1b}$$

where w is the $1/e^2$ beam radius and $P(t)$ is the power of the beam as a function of time. For modeling purposes we assume that for a pulsed laser, $P(t)$ is approximately constant during a pulse and equal to zero between pulses.

We assume an initial condition on Eq. (1a) of $T = T_o$ for $t = 0$ and we assume a boundary condition of $T = T_o$ for $z = \infty$ and $r = b$ where b is the radial boundary. A convective boundary condition of $-\frac{\partial T}{\partial z} + H(T - T_o) = 0$ is assumed at the tissue surface ($z = 0$) where H is the convective constant (cm^{-1}) for the air-tissue interface.

3.2. Separation of the heat-transfer equation

It can be shown that to a good approximation the diffusion terms, $\frac{\partial^2 T}{\partial r^2} + \frac{1}{r}\frac{\partial T}{\partial r} + \frac{\partial^2 T}{\partial z^2}$, can be ignored during the laser pulse when the diffusion time is small ($t = 250$ μs), but between pulses ($t = 200$ ms) the diffusion terms can not be ignored. For a single laser pulse, Eq. (1a) then becomes

$$\mu E(r,t)\exp(-\mu z) = \rho c\frac{\partial T}{\partial t} \tag{2}$$

during a pulse where T = T(r,z,t) is the scleral temperature due to the pulse and

$$\frac{\partial^2 T}{\partial r^2}+\frac{1}{r}\frac{\partial T}{\partial r}+\frac{\partial^2 T}{\partial z^2}=\frac{1}{\alpha}\frac{\partial T}{\partial t} \tag{3}$$

between pulses where T = T(r,z,t) is the temperature resulting from diffusion of time t.

Equations (2) and (3) are referred to as the generation and diffusion equation, respectively. Their solution allows determination of the absorption coefficient and thermal diffusivity of irradiated tissue from surface-temperature measurements.

3.3. Calculation of the absorption coefficient

We assume that the absorption coefficient varies linearly with temperature according to $\mu = \mu_o + \beta T(r,z,t)$. Then the solution to Eq. (2) at r = z = 0 for a single pulse is given by

$$T_f = T(0,0,\tau_p) = T_i \exp\left(\frac{\beta I_o}{\rho c}\right)+\frac{\mu(T_i)}{\beta}\left[\exp\left(\frac{\beta I_o}{\rho c}\right)-1\right] \tag{4}$$

where $\mu(T_i)$ is the absorption coefficient (cm^{-1}) corresponding to the peak surface temperature before the pulse, T_f is the peak surface temperature after the pulse, $I_o = E_o\tau_p$ is the peak fluence of the pulse ($J\ cm^{-2}$), and τ_p is the pulse width (s).

The increase in peak scleral temperature at r = z = 0 due to a laser pulse may be written as $\Delta T_p = T_f - T_i$ where T_f is calculated with Eq. (4) and T_i is the peak surface temperature before the pulse. Furthermore, for a Gaussian beam we assume that the temperature rise throughout the sclera will be given by

$$\Delta T(r,z) = \Delta T_p \exp\left(-2r^2/w^2\right)\exp\left(-\mu(T_i)z\right). \tag{5}$$

Solving Eq. (4) for the absorption coefficient, $\mu(T_i)$, gives

$$\mu(T_i) = \frac{\left[T_f - T_i\exp\left(\frac{\beta I_o}{\rho c}\right)\right]\beta}{\exp\left(\frac{\beta I_o}{\rho c}\right)-1}. \tag{6}$$

An approximate expression for Eq. (6) under the condition $|\beta I_o/\rho c| << 1$ is given by

$$\mu(T_i) = \left[T_f - T_i\right]\left(\frac{\rho c}{I_o}\right) = \Delta T_p\left(\frac{\rho c}{I_o}\right). \tag{7}$$

By measuring the peak surface temperature rise, ΔT_p, due to each pulse, a first estimate for the absorption coefficient as a function of temperature is obtained using Eq. (7). The resulting data is then fit to the line $\mu(T_i) = \mu_o + \beta T_i$ to estimate the slope, β, of the absorption versus temperature curve. The absorption coefficient is recalculated with Eq. (6) and a new estimate for the slope, β, is determined. Equation (6) is resolved and the slope, β, is recalculated until β converges, giving the final absorption coefficient as a function of peak sclera temperature.

3.4. Calculation of the thermal diffusivity

The boundary temperature conditions for Eq. (3) are the same as for the heat-transfer equation given in section 3.1. The initial temperature condition for Eq. (3) is given by the boundary tissue temperature added to the temperature rise in the tissue caused by a laser pulse and is written for the jth pulse as

$$T(r,z) = T_o + \Delta T_j(r,z) = T_o + \Delta T_p \exp\left(-2r^2/w^2\right)\exp\left(-\mu(T_i)\,z\right) \quad \begin{matrix} 0 \le r \le b \\ 0 \le z \le \infty \\ t = 0 \end{matrix}. \tag{8}$$

Equation (3) with its initial and boundary conditions can be solved with a separation of variables technique.[6] For a diffusion time t' after the jth pulse, the solution for a temperature-dependent absorption and thermal diffusivity is given by

$$T(r,z,t) = T_o + T_j(r,z,t') = T_o + \frac{4}{\pi b^2}\Delta T_p \sum_{m=1}^{\infty} \frac{J_o(\beta_m r)}{J_1^2(\beta_m b)} \exp\left(-\alpha(T_f)\beta_m^2 t'\right)$$

$$\times \int_{\eta=0}^{\infty} \exp(-\alpha(T_f)\eta^2 t') \frac{(\eta\cos(\eta z) + H\sin(\eta z))}{(\eta^2 + H^2)(\mu(T_i)^2 + \eta^2)} \eta(\mu(T_i) + H)\,d\eta \tag{9}$$

$$\times \int_{r'=0}^{b} r' J_o(\beta_m r') \exp\left(-2r'^2/w^2\right) dr'$$

where I_o is the peak fluence of the pulse, $\mu(T_i)$ is the absorption coefficient for scleral tissue as a function of peak tissue temperature before the pulse, $\alpha(T_f)$ is the thermal diffusivity for the sclera as a function peak tissue temperature after the pulse, b is the radius at which the boundary tissue temperature is applied, and β_m are the roots of $J_o(\beta_m b) = 0$. The diffusion time, t', is given by $t' = t - t_j$ where t_j is the time at which the pulse is applied and t is time at which the temperature is calculated. It was found that b need only be 3 times the beam radius w and the series over m need only contain 15 terms in order to produce convergence to within 0.5%. The integrals over η and r' can be solved numerically.

The decrease in sclera temperature following each pulse was measured with the thermal-imaging system and was used with Eq. (9) to determine numerically the thermal diffusivity, $\alpha(T_f)$, of scleral tissue. The measured peak temperature drop after each pulse was compared to the decrease calculated with Eq. (9) with r = z = 0. The thermal diffusivity in Eq. (9) was adjusted until the modeled and experimentally measured temperature decreases agreed to within 1%. Using this technique, the thermal diffusivity was determined for the time interval following each pulse and was recorded as a function of the peak surface temperature to yield $\alpha(T_f)$.

3.5. Thermal model for a pulse train

The heat equation for multiple pulses was solved by adding the initial tissue temperature to the temperature response from each pulse with a time delay. The tissue temperature after n pulses can be written:

$$T(r,z,t) = T_o + \sum_{j=1}^{n} T_j(r,z,t-t_j) \tag{10}$$

where T_o is the initial ($t = 0$) tissue temperature, t_j is the time at which the jth pulse is fired, $t' = t - t_j$ is the diffusion time for the jth pulse, and T_j is the temperature response from the jth pulse. The response T_j consists of the temperature rise caused by a pulse and the subsequent temperature drop that results from diffusion and is given by Eq. (9).

The temperature resulting from a series of pulses is obtained by solving Eq. (9) for each pulse and adding the responses with Eq. (10). Temperature distributions were calculated for a range of values of peak fluence, I_o, beam radius, w, and number of pulses, n. The absorption coefficient, $\mu(T_i)$, and thermal diffusivity, $\alpha(T_f)$, were taken from the previously calculated values. The peak surface temperature of scleral tissue as a function of time was calculated by solving Eqs. (9) and (10) as a function of t with $r = 0$ and $z = 0$. To calculate depth temperature profiles that correspond to the maximum temperature reached in the sclera, Eqs. (9) and (10) were solved with $r = 0$ as a function of z for the time, t, immediately after the final pulse is applied.

3.6. Optimum parameters for LSB

Laser scleral buckling was simulated with our thermal model under various treatment parameters (peak fluence, spot size, and number of pulses) and the resulting temperature distributions were compared to predefined damage and shrinkage criteria. For effective LSB treatment, shrinkage temperatures should be reached as deep in the tissue as possible, while minimizing tissue damage. We assume a shrinkage threshold of 60 °C for scleral collagen. We assume damage thresholds of 85 °C for the sclera and 43 °C for the sclera-choroid boundary ($\cong$1 mm). The beam parameters which produced temperature distributions that were within these thresholds and gave the largest shrinkage depths were considered optimal.

4. RESULTS

4.1. Thermal measurements

Figure 2 shows the evolution of peak surface temperature of the sclera as a function of time in one of the trials in which twenty-three pulses were applied to the sclera. The spikes indicate the maximum temperature observed for each laser pulse. A temperature rise is observed in response to successive pulses and a decay is observed for a few seconds after the final pulse. The maximum scleral temperature for the trial is observed to be $99\,^{\circ}C$ and occurs at the twenty-second and twenty-third pulses. This is consistent with the temperature limit for tissue containing water which is $100\,^{\circ}C$.

Figure 3 shows a cross-section of the spatial distribution of the surface temperatures for several laser pulses immediately after each pulse. The distributions are approximately Gaussian. The surface temperature rises rapidly during the first pulses and remains almost constant during the last pulses.

4.2. Accuracy of the measurements

Limitations of the calibration process include issues of system noise and stability. Noise in the image data consists of random pixel variations caused by camera electronics. This produced an rms noise level of about $0.3\,^{\circ}C$ in our measurements. The main stability issue of the camera is a cooler cycle with a period of about 32 s and a temperature range of about $\pm 1\,^{\circ}C$. Another stability issue is a shift in the camera's pedestal position resulting from fluctuations in room temperature or any other stress on the camera's cooling system. Each of these variations was corrected by subtracting from the images the variations of background reference pixels. It was determined that when correcting stability shifts by this method, an rms error of about $0.3\,^{\circ}C$ remains. The total rms error in our temperature measurements was determined from the noise and stability rms errors to be about $0.4\,^{\circ}C$.

4.3. Absorption coefficient for scleral tissue

A first estimate of the absorption coefficient for scleral tissue as a function of peak surface temperature was obtained with Eq. (7). The density, ρ, and heat capacity, c, were taken for a tissue which is composed of 70% water. These values are approximately[7] $\rho = 1.09$ g cm^{-3} and $c = 3.35$ J g$^{-1}\,^{\circ}$C^{-1}. Because the beam profile in the experimental trials was of the form $I = I_o \exp\left(-2r^2/w^2\right)$, the peak fluence is $I_o = 5.0$ J cm^{-2} which is twice the average fluence. Substituting these values for ρ, c, and I_o into Eq. (7) gives

$$\mu(T_i) = \frac{\rho c \Delta T_p}{I_o} \approx 0.73 \times \Delta T_p \qquad (11)$$

The absorption coefficient for scleral tissue was estimated with Eq. (11) for three trials by measuring the peak surface temperature rise, ΔT_p, resulting from each pulse. The calculated absorption coefficient was found to have a nearly linear dependence with temperature. The data was fit to the line $\mu(T_i) = \mu_o + \beta T_i$ by minimizing rms error. The absorption coefficient was then recalculated with Eq. (6) until the measured slope, β, converged to the value used in Eq. (6). Figure 4 shows the resulting

data. The absorption coefficient (cm^{-1}) for scleral tissue at 2.1 μm is found to be given by $\mu(T_i) = -0.1 \times T_i + 28$ where T_i is the peak scleral temperature before absorption. The rms error between this line and the data points is found to be 1.1 cm^{-1}. This curve is found to decrease from 26 cm^{-1} at 20 °C to 20 cm^{-1} at 80 °C. For room temperature, the value is 26 cm^{-1}, which is equal to a previous measurement[8] for the absorption coefficient of corneal tissue.

Previously calculated absorption coefficients[9] for 2.1 μm Ho:YAG irradiation are shown in Fig. 4 for pure water which were calculated from transmission experiments and from spectrophotometer data. It should be noted that the absorption coefficient for scleral tissue is plotted as a function of peak surface temperature during laser irradiation while the absorption coefficient for pure water is plotted as a function of a temperature which is spatially uniform. Figure 4 shows that the absorption coefficient calculated for scleral tissue has a more steeply declining slope than the absorption coefficient for pure water. This may be explained by the dehydration of the tissue with each pulse as water is the main absorber of midinfrared radiation in tissue.

4.4. Thermal diffusivity for scleral tissue

The thermal diffusivity of scleral tissue as a function of peak temperature before diffusion was obtained by measuring the temperature drop after each pulse in three trials and comparing to that calculated with Eq. (9). Equation (9) was solved iteratively for each pulse by adjusting the thermal diffusivity, $\alpha(T_f)$, until the experimental and calculated temperature drops were in agreement. Agreement to within 1% was typically achieved after 5 to 10 iterations. The resulting data for thermal diffusivity versus peak temperature for scleral tissue is shown in Fig. 5. The data points were fit to a straight line by minimizing rms error. The resulting thermal diffusivity for scleral tissue is given by $\alpha(T_f) = -2.2 \times 10^{-5} \times T_f + 2.9 \times 10^{-3}$ in units of $cm^2\ s^{-1}$ where T_f is the peak scleral temperature after a pulse. The rms error between this line and the data points is found to be 1.4×10^{-4} $cm^2\ s^{-1}$. The linear fit decreases from 2.0×10^{-3} $cm^2\ s^{-1}$ at 40 °C to 0.7×10^{-3} $cm^2\ s^{-1}$ at 100 °C. Also shown in Fig. 5 is the thermal diffusivity for pure water as calculated from known values[10] of the density, heat capacity, and thermal conductivity, of water. The more steeply declining slope of the thermal diffusivity versus temperature for scleral tissue is probably a result of the dehydration of the tissue during the LSB procedure as the thermal diffusivity for tissue decreases with decreasing hydration[7]. It should be noted that a constant value of the thermal diffusivity was assumed between pulses. In reality the thermal diffusivity changes continuously as diffusion occurs and the tissue cools. Because the time interval between pulses is small (0.2 s), the error induced by this assumption should be small.

4.5. Thermal models of LSB with various pulse parameters

Equations (9) and (10) were solved with various pulse parameters to generate LSB temperature profiles. Absorption coefficients, $\mu(T_i)$, and thermal diffusivities, $\alpha(T_f)$, were used for each pulse from the previously calculated values. To calculate the peak surface temperature of scleral tissue as a function of time, Eqs. (9) and (10) were solved with $r = 0$ and $z = 0$ as a function of t. To calculate the depth temperature profile, Eqs. (9) and (10) were solved with $r = 0$ as a function of z.

The peak scleral surface and 1-mm-depth temperatures were calculated for various beam parameters. All calculations were made with a convective constant of $H = 5$ cm^{-1} and an initial scleral temperature of 35 °C. Peak scleral surface temperature ($r = 0$ mm, $z = 0$ mm) and the temperature of the sclera at a depth of 1 mm ($r = 0$ mm, $z = 1$ mm) were determined as functions of the number of pulses applied and the average fluence of the beam. A pulse rate of 5 Hz was assumed.

Figure 6 shows the modeled peak scleral surface ($r = z = 0$) temperature responses to 2 pulses from a Ho:YAG laser source as a function of time with an average fluence of 2.5 J cm^{-2}. The beam radii, w, range from to 0.25 to 1.5 mm. The total energies, E, are calculated as $E = \pi w^2 I_{avg}$ and range from 5 to 177 mJ. Figure 7 shows the corresponding temperature as a function of depth ($r = 0$) in the sclera immediately after the second pulse. Figure 7 shows that the shrinkage depth for a beam with a radius of 1 mm is about 0.37 mm and the shrinkage depth for a beam with a radius of 1.5 mm is about 0.4 mm.

4.6. Optimum parameters for LSB

It was found that under the established damage thresholds, the largest obtainable shrinkage depth is about 0.4 mm, which occurs for a fluence of 2.5 J cm^{-2} and 2 pulses. The scleral temperature at a depth of 1 mm for this trial was found to be 43 °C, which is at the threshold of choroidal damage. However because of the cooling effect of blood circulation in the retina, the actual choroidal temperature during surgery would be slightly lower than this. Using a more accurate calculation for the retinal damage threshold will probably result in less restrictive conditions on the peak fluence, beam diameter, and number of pulses that can be used for LSB. With these new parameters, shrinkage depth might be increased without causing thermal damage to the sclera or retina.

5. CONCLUSIONS

IR imaging data of the laser scleral buckling process were collected. From these data, temperature distribution images and plots were generated with 33-ms temporal resolution and 44-μm spatial resolution. The absorption coefficient and thermal diffusivity of scleral tissue and their dependence on temperature were determined from the temperature data. The absorption coefficient was found to vary from 26 to 20 cm^{-1} over the temperature range from 20 to 80 °C and has a more steeply declining slope than previous measurements made for pure water. The thermal diffusivity was found to vary from 2.0×10^{-3} to 0.7×10^{-3} $cm^2\ s^{-1}$ over the temperature range from 40 to 100 °C and has a more steeply declining slope than the thermal diffusivity versus temperature for pure water.

The large variation with temperature of the absorption coefficient and thermal diffusivity indicate the need to use temperature dependent thermal and optical properties in thermal models of pulsed laser tissue heating to prevent significant errors in temperature calculations. In addition, both the absorption coefficient and the thermal diffusivity versus temperature curves for scleral tissue were found to have a more steeply declining slope than for pure water. This may be a result of the reduction of water in the tissue during surgery and suggests that the effects of changing tissue hydration should by included in thermal models of multipulse tissue irradiation.

A thermal model is developed which, based on the measured absorption coefficient and thermal diffusivity, provides a method for generating scleral surface and depth temperatures for various pulse parameters. From this model, temperature responses were generated for LSB procedures performed over a range of fluences and number of pulses. Modeling demonstrated that LSB performed with an average fluence of 2.5 J cm^{-2}, a beam radius of 1 mm, and 2 pulses produces a shrinkage depth of 0.37 mm, which is acceptable for LSB treatment. For these parameters, the peak sclera temperature and the temperature at a depth of 1 mm were below their respective damage thresholds.

This work demonstrates a convenient method for determining the absorption coefficient and thermal diffusivity of ocular tissue with infrared imaging. With appropriate modeling techniques, these methods may be extended to determine other tissue properties such as density, hydration, specific heat, and conductivity. The methods used in this paper may be extended to determine the thermal and optical constants for various wavelengths, tissue types, and surgical processes.

6. ACKNOWLEDGMENTS

The authors are grateful to Jin-Hui Shen for technical assistance. This work was supported in part by the Fight for Sight Division of Prevent Blindness America, by Research to Prevent Blindness, New York, New York, by the Florida Lions Eye Bank, and by the Enterprise Florida Innovation Partnership.

7. REFERENCES

1. Q. Ren, G. Simon, J.M. Parel, and W. Smiddy, "Laser scleral buckling for retinal reattachment," *American Journal of Ophthalmology*, 115: 758-762, 1993.

2. H. Stringer and J. Parr, "Shrinkage temperature of eye collagen," *Nature*, 204: 1307, 1964.

3. E. Spoerl, K. Schmalfuss, U. Genth, T. Seiler, and H.J. Huebscher, "Thermo-mechanical behavior of the cornea," *Investigative Ophthalmology and Visual Sciences*, 36: S39, 1995.

4. M. Sasoh, J.M. Parel, I. Nose, J.H. Shen, J. Comander, and W. Smiddy, "Laser scleral buckling: in-vitro quantification for Ho:YAG and Tm:YAG lasers," *SPIE Proceedings*, 2393: 299-305, 1995.

5. M.J.C van Gemert, A.J. Welch, "Time constants in thermal laser medicine," *Lasers in Surgery and Medicine*, 9: 405-421, 1989.

6. M.N. Ozisik, *Heat Conduction*, 2nd Edition, John Wiley and Sons, 1-130, 1992.

7. A.L. McKenzie, "Physics of thermal processes in laser-tissue interaction," *Phys Med Biol*, 35: 1175-1209, 1990.

8. S. Mitsunaga, H. Hamano, and K. Miyabe, "Thermal Property Measurements of the Cornea," *The First Japanese Symposium on Thermophysical Properties*, 159-162, 1980.

9. E.D. Jansen, T.G. van Leeuwen, M. Motamedi, C. Borst, and A.J. Welch, "Temperature dependence of the absorption coefficient of water for midinfrared laser radiation," *Lasers in Surgery and Medicine*, 14: 258-268, 1994.

10. CRC Handbook of Chemistry and Physics: CRC Press, Boca Raton, pp. D-171, E-10, F10; 1985.

8. FIGURES

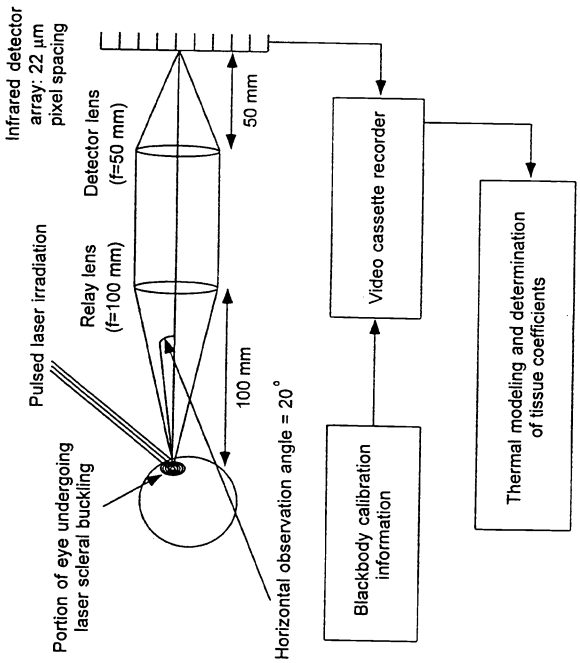

Figure 1: Thermal imaging and data recording setup.

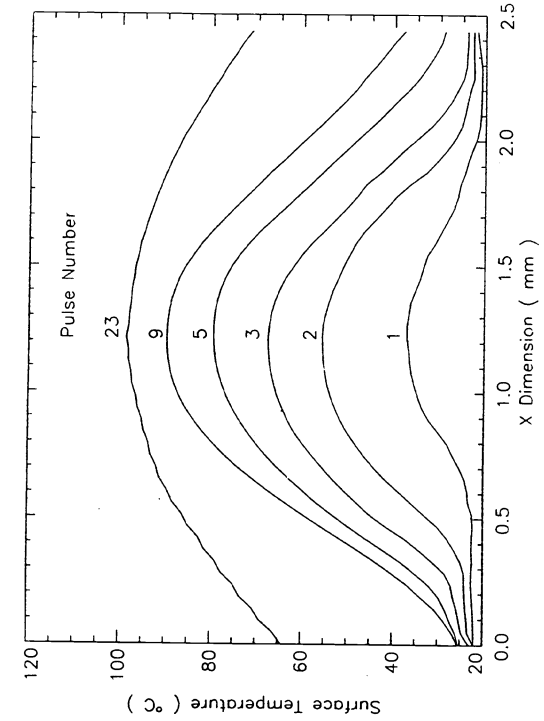

Figure 3: Cross section of the spatial temperature distribution at the surface of the sclera just after the firing of pulses 1, 2, 3, 5, 9, and 23 with a Ho:YAG laser (2.1 µm, 250 µs, 5 Hz, 2.5 J cm^{-2}).

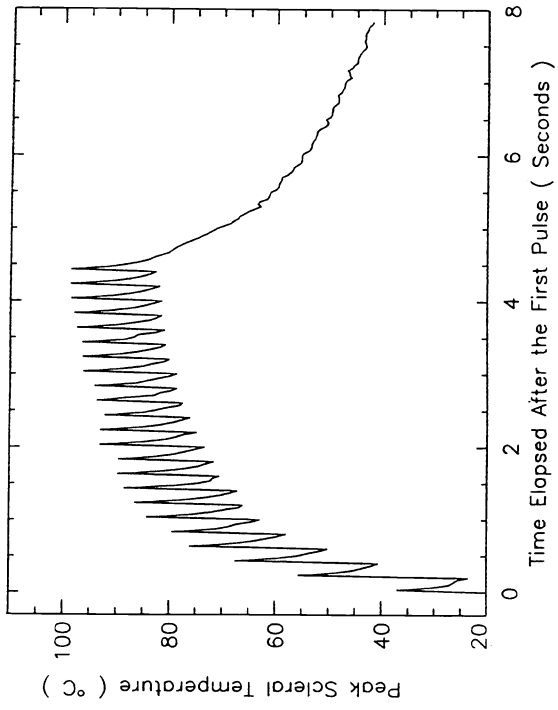

Figure 2: Plot of the peak surface temperature of the sclera as a function of time as twenty-three pulses are fired with a Ho:YAG laser (2.1 µm, 250 µs, 5 Hz, 2.5 J cm^{-2}).

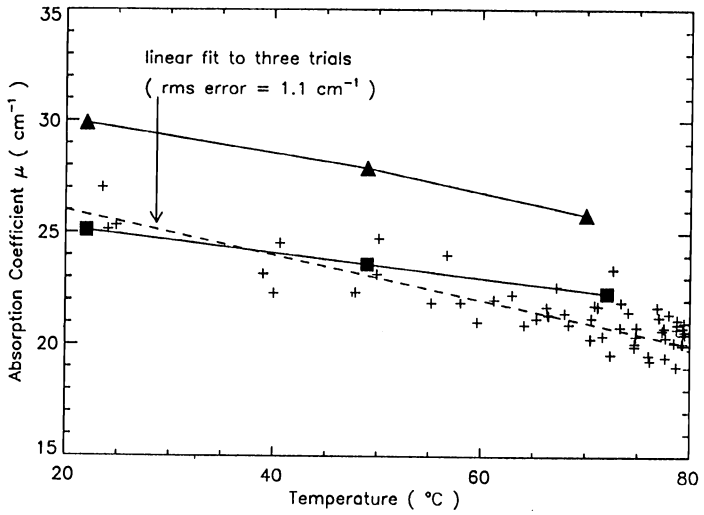

Figure 4: Variation of the absorption coefficient at 2.1 μm with temperature for (- -) scleral tissue, (■) pure water calculated[9] from transmission experiments, and (▲) pure water calculated[9] from spectrophotometer measurements.

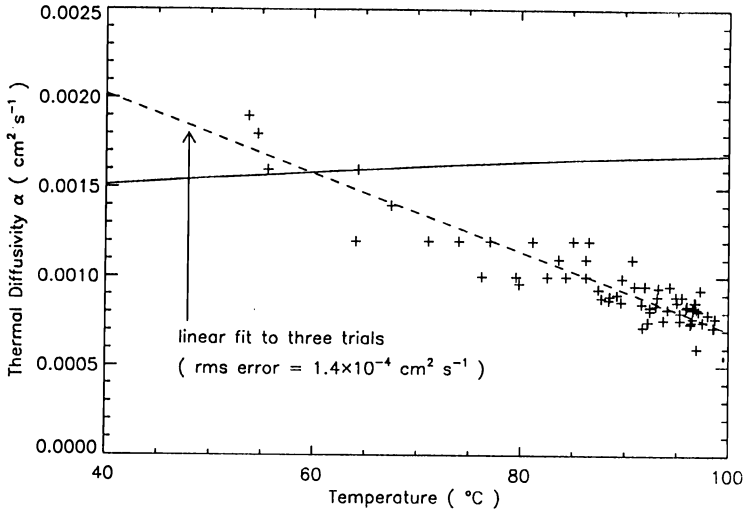

Figure 5: Variation of the thermal diffusivity with temperature for (- -) scleral tissue and (—) pure water calculated from known values[10] of density, heat capacity, and thermal conductivity.

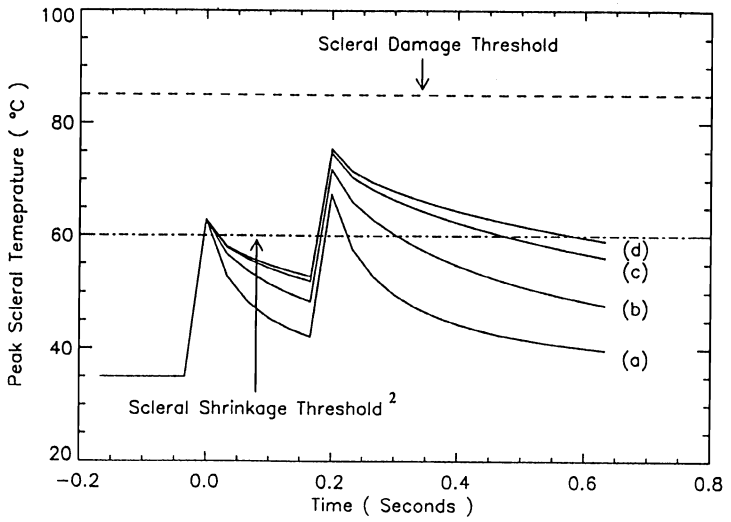

Figure 6: Modeled scleral surface (r = z = 0) temperature response to 2 pulses from a Ho:YAG laser source (5 Hz) with I_{avg} = 2.5 J cm^{-2} and w = (a) 0.25 mm, (b) 0.5 mm, (c) 1.0 mm, (d) 1.5 mm.

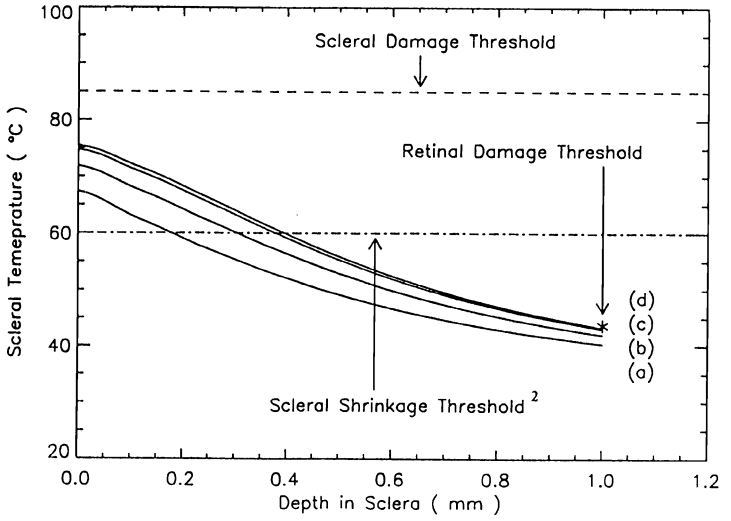

Figure 7: Modeled scleral depth (r = 0) temperature response to 2 pulses from a Ho:YAG laser source (5 Hz) with I_{avg} = 2.5 J cm^{-2} and w = (a) 0.25 mm, (b) 0.5 mm, (c) 1.0 mm, (d) 1.5 mm.